



Design, Simulation, and Optimization of a Meander Micro Hotplate for Gas Sensors

Bedoui Souhir[†], Gomri Sami, Charfeddine Samet Hekmet,
and Kachouri Abdennaceur

Department of Electrical Engineering, National School of Engineer Sfax, University of Sfax, Sfax 3038, Tunisia

Received January 13, 2016; Revised February 23, 2016; Accepted May 9, 2016

Micro Hotplate (MHP) is the key component in micro-sensors, particularly gas sensors. Indeed, in metal oxide gas sensors MOX, micro-heater is used as a hotplate in order to control the temperature of the sensing layer which should be in the requisite temperature range over the heater area, so as to detect the resistive changes as a function of varying concentration of different gases. Hence, their design is a very important aspect. In this paper, we have presented the design and simulation results of a meander micro heater based on three different materials - platinum, titanium and tungsten. The dielectric membrane size is 1.4 mm × 1.6 mm with a thickness of 1.4 μm. Above the membrane, a meander heating film was deposited with a thickness of 100 nm. In order to optimize the geometry, a comparative study by simulating two different heater thicknesses, then two inter track widths has also been presented. Power consumption and temperature distribution were determined in the micro heater's structure over a supply voltage of 5, 6, and 7 V.

Keywords: Gas sensors, Heater, Platinum, Titanium, Tungsten, Electro-thermal analysis

1. INTRODUCTION

Physical and chemical processes of the pollutant gases in the troposphere, particularly nitrogen oxides NO_x and the volatile organic compounds (VOC), result in the formation of secondary oxidized products. As several of these processes are regulated by the presence of sunlight, the oxidized products, including an oxidant such as O₃, are commonly referred to as 'secondary photochemical pollutants'. The production of high levels of ground ozone is of particular concern, because it known to act as the primary source of OH and also as a greenhouse gas. Furthermore tropospheric O₃ exerts adverse effects on human health, vegetation and materials [1]. Monitoring pollutants such as ozone could significantly increase the quality of human life. The only solution was to route the sensor data to the central control-

ler through the wiring. It had several flaws, as well as being expensive and cumbersome. Recent years have seen a great progress in the Internet of Things (IoT) devices and related products such as wireless sensors [2]. In fact, IoT devices receive input environmental data through sensors and send out information through wireless interfaces to computers and mobiles [3]. IoT devices should be designed to minimize power consumption. They also require long lifetime batteries. In fact, in order to reduce power consumption, the sensor will be mostly inactive. Indeed, as the time necessary to attain the high temperature required for gas detection is a few milliseconds, the sensor will be active only for few seconds to detect the gas, after which it will stay in sleep mode for most of the time. The transition to active state will therefore be periodic. As a consequence, monitoring and controlling air quality parameters form an important subject of atmospheric and environmental research today. Gas sensors with low power consumption play an important role in the measurement of gases, mainly for environmental monitoring.

Many researchers have demonstrated the suitability of thin or thick WO₃ films as sensing layers for gas monitoring applications [4,5]. Indeed, to excite the semiconductor-sensitive material, a

[†] Author to whom all correspondence should be addressed:
E-mail: souhir.bedoui@yahoo.fr

Copyright ©2016 KIEEME. All rights reserved.

This is an open-access article distributed under the terms of the Creative Commons Attribution Non-Commercial License (<http://creativecommons.org/licenses/by-nc/3.0>) which permits unrestricted noncommercial use, distribution, and reproduction in any medium, provided the original work is properly cited.

certain operating temperature is needed to achieve good sensing properties [6]. A large number of studies demonstrated that tungsten dioxide WO_3 expose a high sensitivity, particularly to ozone [7]. These sensors work at high temperatures (197~447 °C) [8]. Micro hotplate (MHP) is one of the main components to maintain the required temperature for detecting the gases. The latter allows high sensitivity, high selectivity, lower power consumption, small size and compatibility with semiconductor devices [9].

The number of applications for micro-heater devices is growing rapidly, as they are key components in subminiature micro-sensors such as gas sensors. The main objective of a wide range of research is miniaturized gas sensors with low power consumption. In fact, the majority of gas sensitive materials operate at elevated temperatures. In metal oxide gas sensors MOX, micro-heater is used as a hotplate in order to control the temperature of the sensing layer [10]. Micro Hotplate consists of a thermally isolated stage with a heater structure, a temperature sensor and a set of contact electrodes for the sensitive layers. Using this Microstructure architecture (topology, structure), high operation sensors can be made, ensuring comparably low power consumption [11]. Micro heater is appreciated since it allows the reduction of the sensor power consumption and enables in temperature modulation of the gas sensing, which results in an improvement of gas selectivity performance [12]. Hence, their design is a very important aspect and choosing the perfect material is a challenge for the enhanced performance of the gas sensor.

In this study, we report on the design and electro-thermal simulation of micro-heaters used in gas sensors. The design is optimized for low power consumption and better temperature uniformity. Simulations have been carried out using a finite element analysis. Power consumption of the platinum heater is compared with titanium and tungsten heater.

2. EXPERIMENTS

2.1 Mathematical formulation

The electro-thermal simulation provides coupling electrical and thermal behavior. In the framework of this simulation, we used the electro-thermal model to simulate heating by Joule effect. This model includes two modes: conduction mode with the continuity equation is given by equation (1), and heat transfer mode is represented by equation (2) [15].

$$-\nabla \cdot (\sigma \cdot \nabla V) = 0 \quad (1)$$

$$\rho_v \cdot C_p \frac{\partial T}{\partial t} - \nabla \cdot (k \cdot \nabla T) = Q \quad (2)$$

These two equations are linked by the following equation of Joule heating [15]:

$$Q = \sigma |\nabla V|^2 \quad (3)$$

Where ρ_v is the density of heater material, C_p is the heat capacity at constant pressure of heater material, k is the thermal

conductivity of the heater material, and ∇V is the potential difference across the heater material.

The simulations are carried out at a variable voltage which was applied to one end of the heating electrode, while the other end is grounded.

The electric conductivity varies with T over a temperature range. This variation is governed by the following equation [14]:

$$\sigma = \frac{\sigma_0}{1 + \alpha(T - T_0)} \quad (4)$$

Where σ_0 is the conductivity at the reference temperature T_0 and α is the temperature coefficient of resistivity. The power consumption is described by the following equation:

$$P = \frac{V^2}{R} \quad (5)$$

Where V is voltage and R is the resistance of heating electrode. Power consumption is directly proportional to the applied voltage and inversely proportional to the resistance of the material.

A resistance of thin micro heater can be found by using the following equation:

$$R = \rho \frac{L}{w \times e} \quad (6)$$

Where ρ is the resistivity of material, L is the length, w is the width, and e is the thickness.

2.2 Design of heater

Figure 1 presents different layers constituting the gas sensor. In fact, the micro-hotplates consist of a heater piled between a membrane and an insulating layer covered with electrodes.

To achieve a desired temperature uniformity and overall sensor performance, the heater design is of great importance. Hence, heater geometry and material have to be chosen carefully. Uniform temperature distribution over the heater surface may be provided using a high thermal conductivity film [14]. Three different metals were used as the heating element, with a thickness of 0.1 μm . The heating film was supported by a silicon dioxide membrane of size 1.4 \times 1.6 mm. In fact the membrane is used as a high temperature electrical insulator to achieve uniform heat distribution over the geometry [15]. This membrane was designed to be very thin (1.4 μm) in order to reduce the conduction losses, since membrane thickness directly affects the performance of the micro hotplate [16]. Micro heater material choice is determined by an operating temperature range suited to the needs, and good homogeneity on the active surface. Platinum (Pt) presents various advantages such as lower density, good specific heat capacity, high electrical conductivity, etc. It is also a dense, malleable, ductile, precious, gray white transition metal. The platinum can be considered as one of the rarest elements in the earth's crust, since it has an average abundance of approximately 5 $\mu\text{g}/\text{kg}$. Thus, it is the least reactive metal. It also has very good specific heat and heating properties. By reducing the dimensions of the geometry,

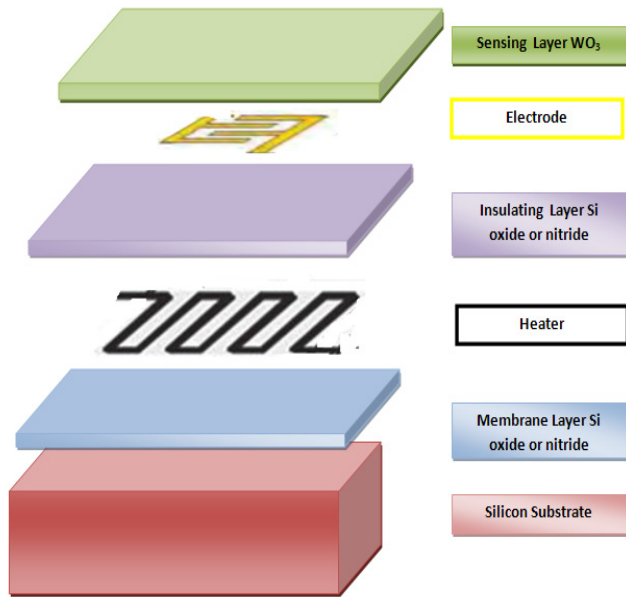


Fig. 1. Top view of gas sensor.

Table 1. Properties of materials used in simulations [18,20-22].

Material	Heat capacity at constant pressure Cp (J.Kg-1 .K-1)	Density ρ_v (kg.m-3)	Thermal conductivity k (W.m-1 .K-1)	Electric resistivity ρ (Ω .m)
SiO ₂	1,000	2,200	1.4	1e12
Pt	130	21,450	71.6	10.6e-8
Ti	522	4,506	21.9	42e-8
W	140	19,300	177	5e-8

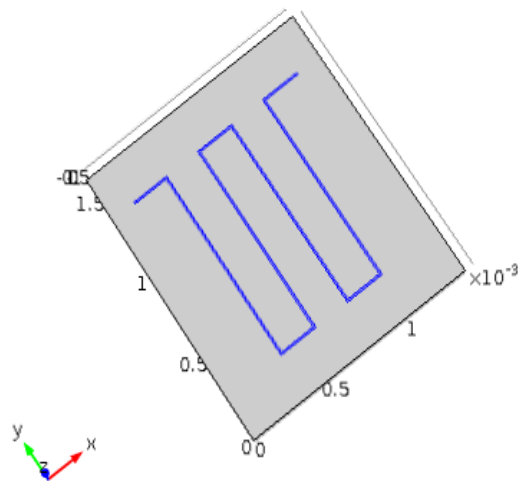


Fig. 2. Heater model.

higher temperature can be achieved [17].

Tungsten (W) has good mechanical strength, and can operate reliably at high temperatures [18]. Titanium (Ti) layer is usually added to improve adhesion of the heater thin film [19]. Material properties are necessary to solve the mathematical equations.

In Table 1 material properties of SiO₂, Pt, Ti and W are shown, respectively. Meander geometry was chosen for our application (Fig. 2). Indeed, this structure could distribute the warmth more uniformly over the heater area, thus reducing the central hotspot [23].

3. RESULTS AND DISCUSSION

3.1 Effect of material micro heater choice for gas sensors

Heater geometry was analyzed by applying different potential to heater contacts (5, 6, and 7 V). Three different heater materials (Pt, Ti and W) were simulated. In order to minimize the modeling error, meshing is an important step for the simulation [24].

Figure 3 consisted of the creation of the 3D finite element mesh. The results of simulation studies showing the temperature distribution over the heater structure are shown below.

Figure 4 represent the simulated result of platinum for 7 volts

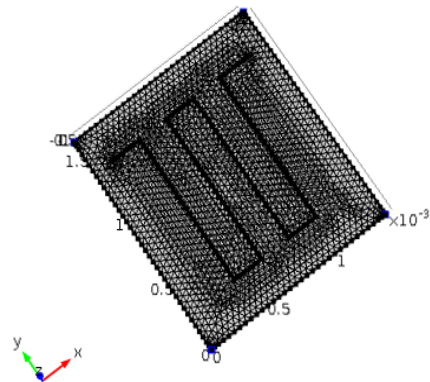


Fig. 3. Meshed model.

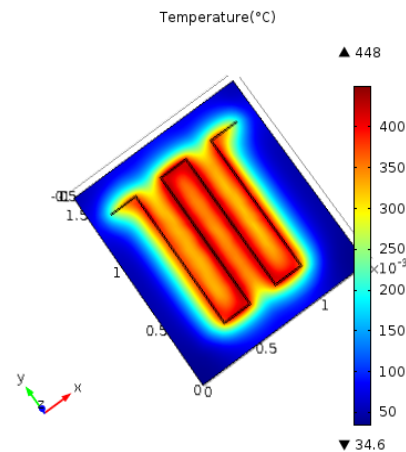


Fig. 4. Temperature distribution in platinum heater at 7 V.

Table 2. Simulation results of heater geometries for different materials.

Material	Voltage (V)	Temperature max (degC)	Average Temperature (degC)	Power consumption (mW)
Pt	5	242	219.02	43.19
	6	336	303.57	62.2
	7	448	403.50	84.66
Ti	5	90.1	83.22	12.04
	6	118	108.02	17.35
	7	151	137.34	23.61
W	5	506	455.40	91.57
	6	716	643.97	131.86
	7	965	866.81	179.48

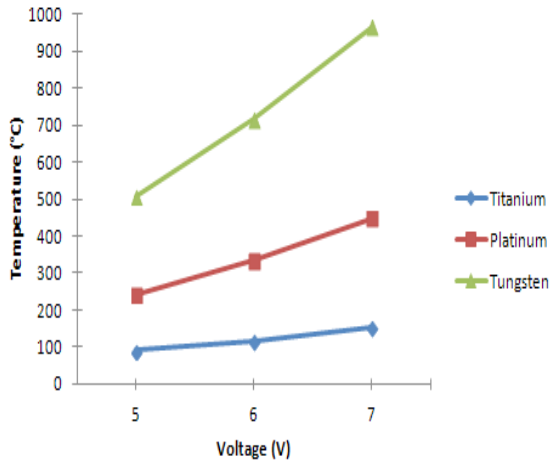


Fig. 5. Maximum temperature VS applied voltage for different heater material.

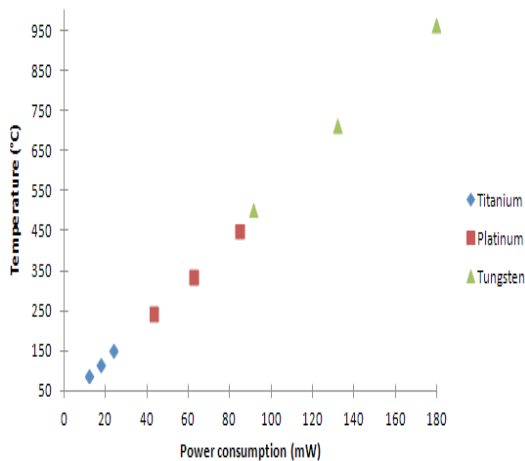


Fig. 6. Temperature VS power consumption for different heater material.

input. Electro-thermal simulation of heating electrode of various materials and various voltages, and their corresponding power consumptions are shown in Table 2.

Platinum used for heating element is compared with titanium and tungsten at 5, 6, and 7 V (Fig. 5 and 6). We found that Titanium has low power consumption as compared to tungsten and platinum, due to its high resistivity and low thermal conductivity. But the temperature over the active area still weak of around 151 °C for 7 V input voltage. However, tungsten had the highest power consumption due to its low resistivity and high thermal conductivity. This material ensures a high temperature (about 965 °C) for 7 V input voltage. However, the high power consumption reduced the lifetime of the sensor. Platinum provided a tradeoff between the temperature and power consumption.

In a design of optimized gas sensor, power consumption must be as low as possible and heat losses of the heater must thus be minimized. When the micro hotplate achieves a steady state temperature, electric power consumption must be equal to the heat loss [25]. In fact, the electric power applied to the heater is dissipated by three mechanisms: heat conduction to the structure surrounding the micro hotplate, heat conduction to the air (convection) and radiation. This last is negligible in devices operated at elevated temperatures and will not be regarded [26].

As the layers constituting the device are very thin, conduction is also negligible compared to convection. The heat dissipated through convection is described by the next equation [27]

$$\bar{q}_{convection} = h.s.(T1 - T2) + \Delta h(T)(T1 - T2) \tag{7}$$

Where h: convection coefficient (W.m⁻².K-1), this coefficient can be a temperature dependant coefficient (non linear part) and/or a purely computational quantity.

S: surface area of device in contact with the ambient environment (m²)

T1 and T2 are the temperatures of the surface of the device and the surrounding environment, respectively (K).

In fact, in our stationary study, we considered the heat transfer coefficient as a constant value. On the upper and lower surfaces of the membrane, the heat is dissipated through convective exchange with the gaseous phase. In our design, the air above the membrane was replaced by a generic heat flux boundary condition with a convection coefficient under the dielectric membrane h = 62.5 W/m².K, a convection coefficient over the dielectric membrane h = 125 W/m².K, and a thermal insulation on the rest of the model. Indeed, literature also shows similar values [28,29]. The equation describing the heat dissipated through convection is then as follow:

$$\bar{q}_{convection} = h.s.(T1 - T2) \tag{8}$$

Next table summarizes heat losses and temperature variation for each heater material.

When the temperature increases thermal dissipation gets increases as seen in next figure.

Table 3. Heat losses for different materials.

Material	ΔT(°C)	Heat losses (mW)
Pt	215	41.11
	309	59.20
	421	80.58
Ti	63	12
	91	17.29
	124	23.54
W	479	88.39
	689	129
	938	177

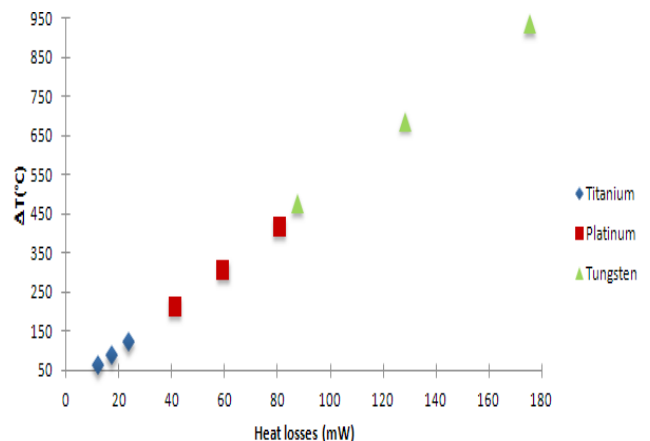


Fig. 7. TVS heat losses for different heater material.

3.2 Effect of micro heater thickness

In this section, a platinum heater was analyzed by applying different potential to heater contacts (5, 6, and 7 V). Two different heater thickness ($e=0.1 \mu\text{m}$ and $e=0.15 \mu\text{m}$) were simulated. Electro thermo simulation of platinum heating electrode at various thicknesses and various voltages, and their corresponding power consumptions, are shown in Table 4.

As the voltage was varied from 5 to 7 V in increments of 1 V, the temperature increased exponentially, and different maximum temperatures were obtained (Fig. 8). Decreasing the thickness of the micro heater means increasing resistance; this lead to a decrease in power consumption, subsequently decreasing the

Table 4. Simulation results of heater geometry for different thicknesses.

Thickness of the heater	Voltage (V)	Temperature max (degC)	Average Temperature (degC)	Power consumption (mW)
0.1 μm	5	242	219.02	43.19
	6	336	303.57	62.2
	7	448	403.50	84.66
0.15 μm	5	348	314.19	64.79
	6	489	440.62	93.30
	7	656	590.04	127

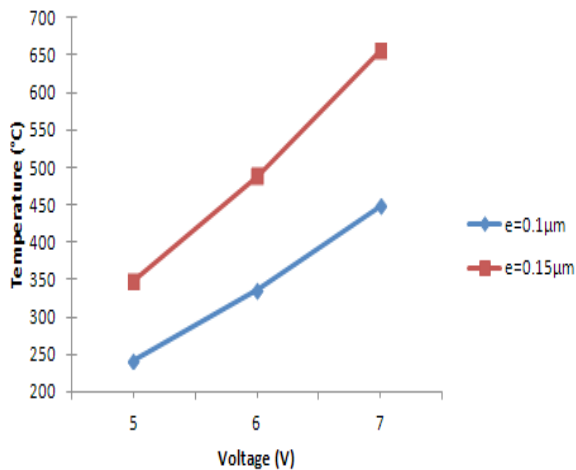


Fig. 8. Maximum temperature VS applied voltage for $e = 0.1 \mu\text{m}$ and $e = 0.15 \mu\text{m}$.

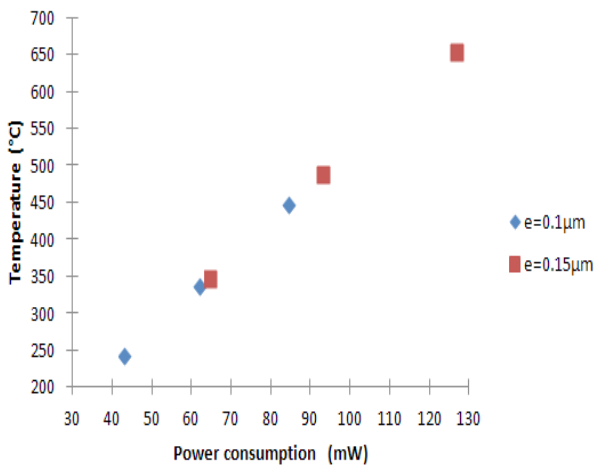


Fig. 9. Temperature vs power consumption for $e = 0.1 \mu\text{m}$ and $e = 0.15 \mu\text{m}$.

heating temperature.

The simulation results presented in Fig. 8 and 9 show that as the thickness of the heating element are increased from $0.1 \mu\text{m}$ to $0.15 \mu\text{m}$, the power consumption of the heater increases from 84.66 mW to 127 mW at 7 V, and the temperature increases from 448°C to 656°C .

3.3 Effect of inter track width

Besides choosing a stable material at high temperature, it is very important to maintain good homogeneity on the active surface. This homogeneity is defined as follow [30]:

$$H = \frac{S_{T_{\text{max}}-40}}{S_{\text{total}}} * 100 \tag{9}$$

Where: $S_{T_{\text{max}}-40}$ corresponds to the area of active surface where the temperature is higher than maximum temperature minus

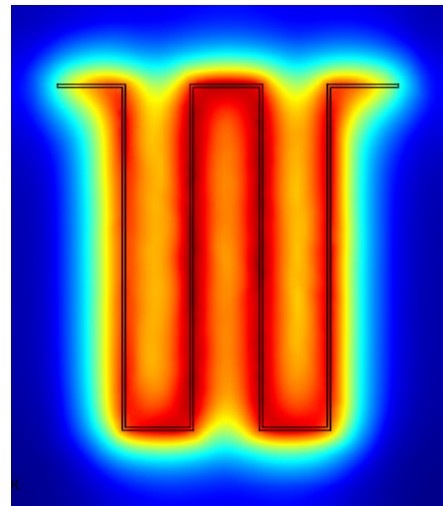


Fig. 10. Temperature distribution in platinum heater at 7 V with $d=0.2 \text{ mm}$.

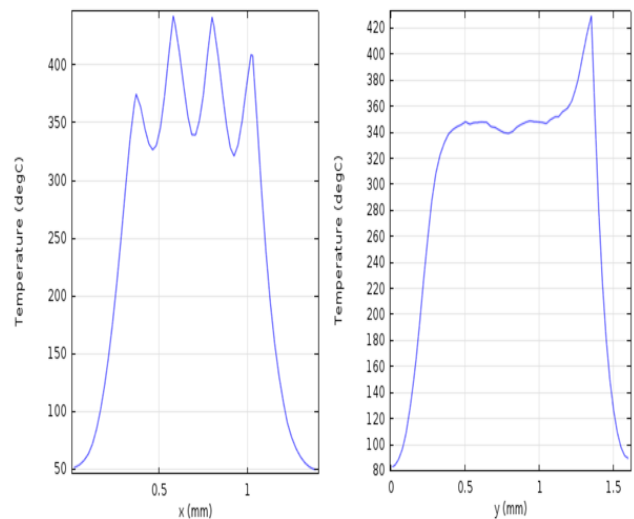


Fig. 11. Temperature profile along x and y axis in platinum heater at 7 V with $d=0.2 \text{ mm}$.

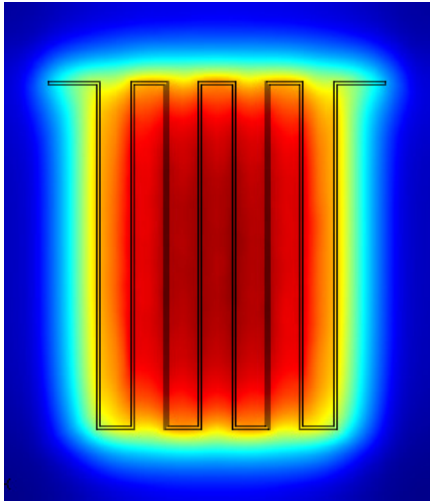


Fig. 12. Temperature distribution in platinum heater at 7 V with $d=0.1$ mm.

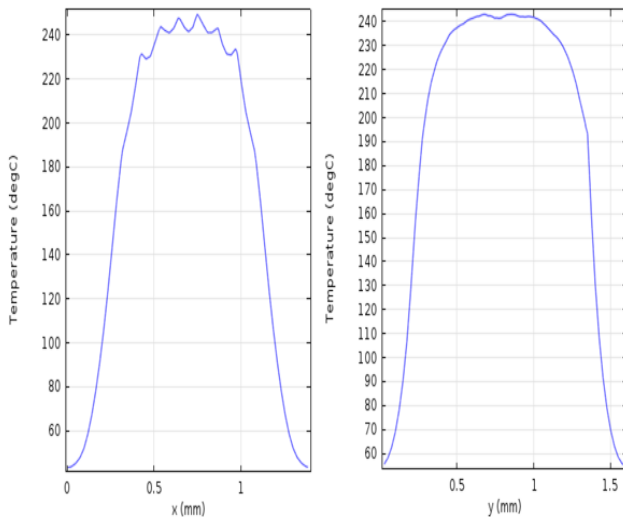


Fig. 13. Temperature profile along x and y axis in platinum heater at 7 V with $d=0.1$ mm.

40 °C, and S_{total} corresponds to the area of active surface.

We performed optimizations on the geometry of the heater in order to improve the homogeneity of the temperature on the surface. The inter-track width was reduced from 0.2 mm to 0.1 mm. Simulation results performed for 7 V are shown in Fig. 10 and 12.

Figure 11 and 13 compares the temperature profiles of two simulated structures (the initial structure with inter track width $d=0.2$ mm, and the structure with inter track width $d = 0.1$ mm). We found that decreasing the inter track width results in homogeneity of the temperature on the surface of 1.1 mm. In fact, the temperature uniformity on this surface increase from 9.52% for $d = 0.2$ mm, to 57.85% for $d = 0.1$ mm.

4. CONCLUSIONS

In this study, three different material thin films (platinum, titanium and tungsten) were used as the heating element for a micro-heater design for use in semiconductor gas sensors. Meander geometry was studied. The effect of the heating element

material on the maximal temperature and power consumption of the heater was evaluated. Platinum offers a compromise between high temperature and power consumption. Subsequently, a platinum thin film was used as the heating element for a micro-heater design for use in semiconductor gas sensors. The effect of various thicknesses of the heating element on the maximal temperature and power consumption of the heater was evaluated. We conclude that if the thickness of the heating electrode is increased from 0.1 to 0.15 microns, then power consumption also increases from 84.66 mW to 127 mW at 7 V voltage, and the temperature increases from 448 °C to 656 °C. Also, in order to improve the homogeneity of the temperature on the surface, we concluded that decreasing the inter track width results in this homogeneity. Hence, the design of the heater and the material used very important aspects. Other geometries will be designed and simulated in prospective works.

REFERENCES

- [1] L. Malec and F. Skacel, *Atmosfera*, **21**, 3 (2008).
- [2] L. Atzori, A. Iera, and G. Morabitoet, *Comput. Netw.*, **54**, 2787 (2010). [DOI: <http://dx.doi.org/10.1016/j.comnet.2010.05.010>]
- [3] D. Miorandi, S. Sicari, F. Pellegrini, and I. Chlamtac, *Ad Hoc Netw.*, **10**, 1497 (2012). [DOI: <http://dx.doi.org/10.1016/j.adhoc.2012.02.016>]
- [4] D. S. Lee, S. D. Han, J. S. Huh, and D. D. Lee, *Sens. Actuat. B Chem.*, **60**, 57 (1999). [DOI: [http://dx.doi.org/10.1016/S0925-4005\(99\)00244-0](http://dx.doi.org/10.1016/S0925-4005(99)00244-0)]
- [5] R. Faleh, M. Othman, S. Gomri, and K. Aguir, *IEEE Sensors J.*, **16**, 3123 (2016). [DOI: <http://dx.doi.org/10.1109/JSEN.2016.2521578>]
- [6] J. Y. Leng, X. J. Xu, L. Y. Ning, H. T. Fan, and T. Zhang, *J. Colloid Interf. Sci.*, **356**, 54 (2011). [DOI: <http://dx.doi.org/10.1016/j.jcis.2010.11.079>]
- [7] M. Bendahan, R. Boulmani, J. L. Seguin, and K. Aguir, *Sensor Actuat B-Chem.*, **100**, 320 (2004). [DOI: <http://dx.doi.org/10.1016/j.snb.2004.01.023>]
- [8] K. Aguir, C. Lemire, and D.B.B. Lollman, *Sensor Actuat B-Chem.*, **84**, 1 (2002). [DOI: [http://dx.doi.org/10.1016/S0925-4005\(02\)00003-5](http://dx.doi.org/10.1016/S0925-4005(02)00003-5)]
- [9] H. Kumar, K. K. Sing, N. Sood, A. Kumar, and R. K. Mittal. Sensors Applications Symposium (SAS) (2014). [DOI: <http://dx.doi.org/10.1109/SAS.2014.6798942>]
- [10] Monika and A. Arora, *International Journal of Advanced Research in Computer Engineering & Technology (IJARCET)*, **2**, 8 (2013).
- [11] N. Kumar and N. Mehta, *Int. J Eng Sci.*, **4**, 7 (2015).
- [12] G. Velmathi, S. Mohan, and N. Ramshanker, *International Journal of Emerging Trends in Electrical and Electronics*, **5**, 2 (2013).
- [13] V. Bansal, A. Gurjar, D. Kumar, and B. Prasad, Excerpt from the Proc. of the COMSOL Conference (Bangalore, 2011).
- [14] V. S. Amrita, Ph. D. *Disertation* (University Ottawa Ontario 2015) p. 50.
- [15] J. Kathirvelan and R. Vijayaraghavan, *J. Eng. Appl. Sci.*, **9**, 11 (2014).
- [16] G. Saxena and R. Paily, *Microsyst Technol.*, **21** (2015). [DOI: <http://dx.doi.org/10.1007/s00542-014-2337-y>]
- [17] N. Kumar and N. Mehta, *International Journal of Engineering Sciences & Research Technology*, **4**, 7 (2015).
- [18] Z. Syed Ali and F. Udrea, W. I. Milne, and J. W. Gardner, **17**, 6 (2008)[DOI: <http://dx.doi.org/10.1109/JMEMS.2008.2007228>]
- [19] A. Z. Sadek, W. Wlodarski, K. Kalantar-zadeh, D. A. Powell, W. L. Hughes, B. A. Buchine, and Z. L. Wang, *Proc. of the Fourth IEEE Sensors 2005 Conference* (Irvine, 2005)[DOI: <http://dx.doi.org/10.1109/ICSENS.2005.1597956>]

- [20] V. K. Khana, M. Parasad, V. K. Dwivedi, C. Shekhar, A. C. Pankaj, and J. Basu, *Indian J Pure Ap.*, 45 (2007).
- [21] T. Guan and R. Puers, *Procedia Engineering*, 5 (2010)[DOI: <http://dx.doi.org/10.1016/j.proeng.2010.09.366>]
- [22] S. Sinha, S. Roy, and C. K. Sarkar, *International Journal of Computer Applications IJCA* (2011).
- [23] G. Velmathi, N. Ramshanker and S. Mohan, *Excerpt from the Proc. of the COMSOL Conference* (India, 2010)
- [24] N. Petra, J. Zweck, S. E. Minkoff, A. A. Kosterev, and J. H. Doty Siam, *J. Appl. Math.*, 71, 1 (2011)[DOI: <http://dx.doi.org/10.1137/100807181>]
- [25] M. Alfredo, J. L. Gonz', and A. Tavira-Fuentes, *Rev. Mex. Fis.*, 54, 1 (2008).
- [26] J. H. Tsai and L. Lin, *J. Microelectromech S.*, 11, 6 (2002)[DOI: <http://dx.doi.org/10.1109/JMEMS.2002.802909>]
- [27] C. A. Wrobel and Brebbia, *Boundary Element Methods in Heat Transfer* (Springer Science & Business Media, 2012) p. 90.
- [28] H. Chalabi, Ph. D. *Disertation*, p. 60, University Paul Cézanne, Tunisian (2007).
- [29] P. Yoboue, Ph. D. *Disertation*, p. 60, University Toulouse, French (2010).
- [30] P. Yoboue, Ph. D. *Disertation*, p. 28, University Toulouse, French (2010).